Tailoring of electric dipoles for highly directional propagation in parity-time-symmetric waveguides

Alice De Corte [*] and Bjorn Maes

Micro- and Nanophotonic Materials Group, Research Institute for Materials Science and Engineering,
University of Mons, 20 Place du Parc, B-7000 Mons, Belgium

Photonic structures offer a flexible platform for studying and demonstrating parity-time ($\mathcal{PT}$) symmetry phenomena. In these platforms, electric dipoles are often used as accurate models for electromagnetic sources, and elliptical dipoles were shown to provide for directional mode excitation. Here we introduce tailored dipole sources for directional excitation in a $\mathcal{PT}$-symmetric structure made of two coupled waveguides. By eliminating one mode in the device, a qualitatively different wave propagation on the two sides of the dipole is achieved. Interestingly, before the exceptional point, a linear dipole suffices to have mode beatings on only one side. Furthermore, beyond the exceptional point, gain can be created on one side only. Finally, at the exceptional point, a near-complete directionality can be achieved due to the mode merging. We explain these effects via a detailed analysis of the modes, and the subsequent mode excitation of the dipole is analytically described. In the end, these various types of contrasting phenomena offer possibilities for integrated photonics applications, routing setups, and lasing behavior.

I. CONTEXT

Electric dipole sources have been used for several years in integrated photonics as compact electromagnetic sources, due to their efficient coupling to photonic guided modes [1–9]. The near-field directionality of elliptically polarized electric dipoles has recently been demonstrated, by taking advantage of constructive or destructive interference of the evanescent waves [1,2,6,9]. Coupling dielectric or plasmonic waveguides to these circular or elliptical dipoles can lead to directional excitation of the waveguide modes, an interesting feature for integrated photonic structures. However, the near field of these elliptical electric dipoles still exhibits an inversion symmetry, which removes the directionality if the dipole is at the center of an inversion-symmetric photonic structure. In order to restore the directional properties between the two sides, we take advantage of the unique characteristics of parity-time-symmetric coupled waveguides.

Parity-time ($\mathcal{PT}$) symmetry has been extensively studied and utilized in photonic structures for several years [10–22]. It can be realized in coupled waveguides by using a balanced profile of the imaginary part of the refractive index, such as two waveguides of identical geometry with one made of an electromagnetic gain material and the other with an equal amount of loss [10–13]. The uniqueness of these $\mathcal{PT}$-symmetric waveguides stems from the two regimes in which they can operate depending on the value of the gain-loss parameter γ, defined by the absolute imaginary part of the refractive index in the waveguides. The transition between these two regimes occurs at the exceptional point (EP), which is located at a certain value of γ dependent on the structure geometry. In the $\mathcal{PT}$-symmetric regime ($\gamma < \gamma_{\mathrm{EP}}$), both supermodes of the structure propagate without any gain or loss, whereas in the $\mathcal{PT}$-broken regime ($\gamma > \gamma_{EP}$) one supermode benefits from the gain and explodes in amplitude, while the other experiences losses and exponentially decays.

The field profile of the modes in $\mathcal{PT}$ structures also has special characteristics. In non-$\mathcal{PT}$ coupled waveguides, the modes have an elliptical in-plane field with ellipse axes that are longitudinal and transverse to the propagation direction [3,4]. When the waveguides present gain and loss in a $\mathcal{PT}$-symmetric fashion, the polarization ellipse of the modes is rotated compared to non-$\mathcal{PT}$ modes [5]. This orientation of the field when $\gamma \neq 0$ needs to be taken into account when coupling with a dipole source, but can also be exploited to obtain unusual coupling relationships when used in combination with the mode symmetries.

In this work, we take advantage of the characteristics of such a $\mathcal{PT}$-symmetric structure with tailored dipoles to create various types of left-right contrasted wave propagation. The results are strongly influenced by the nontrivial, complex nature of the mode profiles in the gain-loss waveguides. In the $\mathcal{PT}$-symmetric regime, due to the careful positioning of the dipole that exploits the polarization of the $\mathcal{PT}$ modes, a *linear* source polarization can be used to obtain beating on only one side of the source. In the $\mathcal{PT}$-broken regime, an elliptical dipole directionally excites the gain mode of the structure, resulting in a unidirectional field amplification. The latter contrast leads to a huge amplitude difference after propagation over a certain length.

The paper is structured as follows. In Sec. II the $\mathcal{PT}$-symmetric coupled waveguide structure is described and its modes are characterized in both $\mathcal{PT}$-symmetric and $\mathcal{PT}$-broken regimes. The coupling of a dipole source to the photonic modes is studied in Sec. III, both in general and in

---

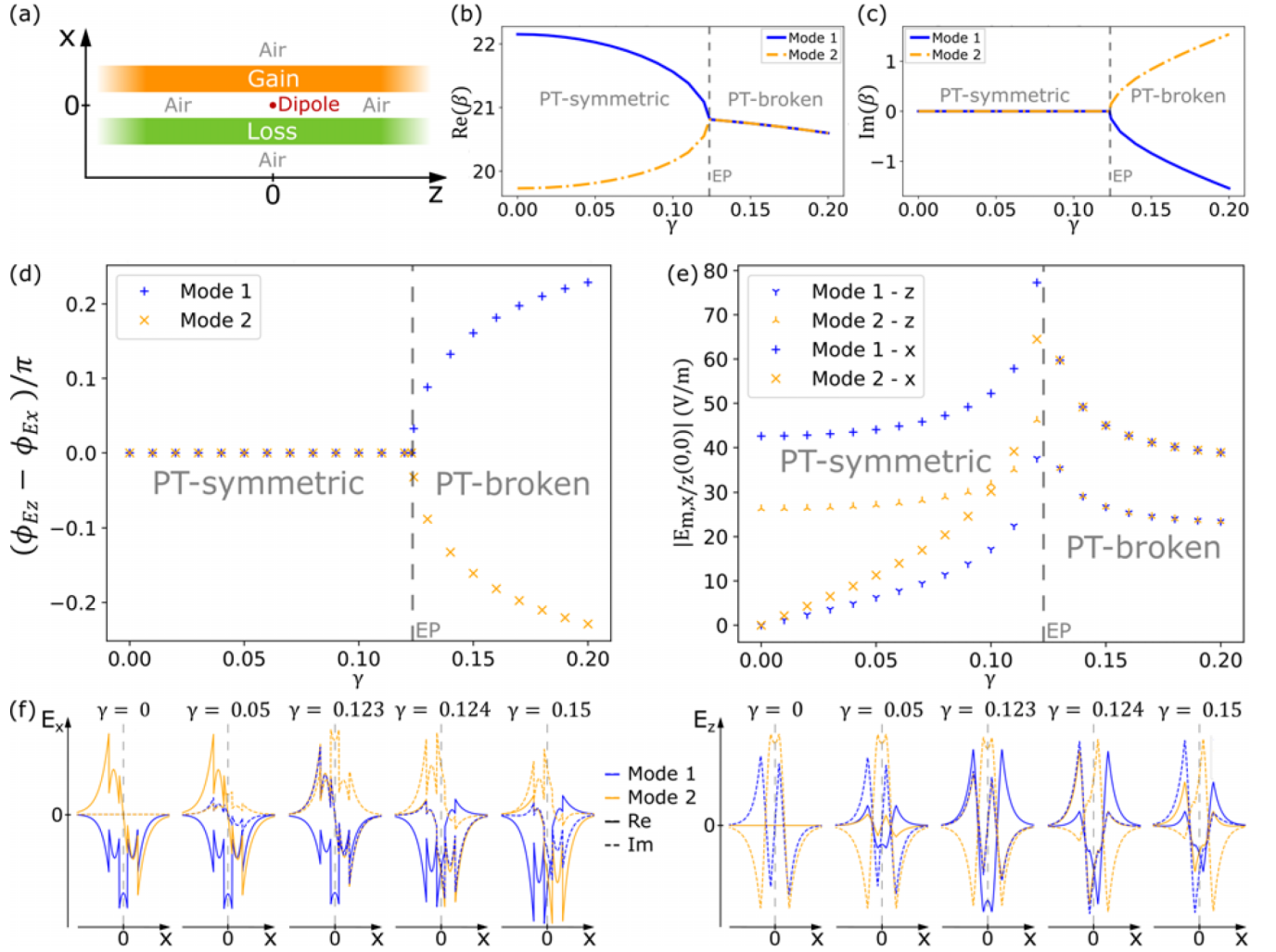[*]Corresponding author: alice.decorte@umons.ac.be

FIG. 1. (a) Schema of the photonic structure used in the simulations. The dielectric gain and loss materials are represented in orange and green, respectively, and the air in white. The waveguides are infinite in the left and right directions ($z \to -\infty$ and $z \to +\infty$). The location of the dipole at (0,0) is marked by a red dot. (b) Real and (c) imaginary propagation constant β (in rad/μm) of modes 1 (blue, full curve) and 2 (orange, dot-dashed curve) of the $\mathcal{PT}$-symmetric structure as a function of the gain-loss parameter γ. The exceptional point is located at $\gamma_{EP} = 0.1231$ and marked by a gray dashed line. (d) Phase difference and (e) module of the x and z electric field components of modes 1 (blue) and 2 (orange) at the dipole location for $\gamma = 0$ to 0.20. The phase difference is calculated as $\phi_{Ez} - \phi_{Ex}$. (f) Electric field profiles of the guided supermodes for $\gamma = 0, 0.05, 0.123, 0.124,$ and 0.15, for both electric components (x and z). The gray dashed line marks the dipole location, $x = 0$

our structure, in order to design an adequate dipole for contrast. Finally in Sec. IV the results of our tailored contrasting dipole are explored.

II. PHOTONIC STRUCTURE CHARACTERIZATION

A. Structure geometry

In our two-dimensional structure, an electric dipole is placed at the center of the air layer separating two $\mathcal{PT}$-symmetric slab waveguides. The dipole is oriented in the simulation plane [xz in Fig. 1(a)]; the relevant modes of our structure are thus the transverse magnetic (TM) modes, with in-plane electric field components and a normal magnetic field component. The waveguide with gain material is at the top, and the lossy guide is at the bottom [see Fig. 1(a)]. The gain and loss materials are characterized by a refractive index of $2 + i\gamma$ and $2 - i\gamma$, respectively, so γ, the gain-loss parameter,

is here the imaginary part of the index (not to be confused with an effective, integrated coefficient).

We use the CAMFR (CAvity Modeling FRamework) eigenmode expansion Maxwell equations solver to numerically simulate our setup for different values of γ [23,24]. The norm of the dipole moment $\vec{p}$ is set to 1 for all configurations. For the calculations, we employed a waveguide thickness of 100 nm, a separation of 80 nm in between, and a vacuum wavelength of 400 nm. However, since the Maxwell equations are scale invariant, the same results are obtained for larger wavelengths by scaling the geometry accordingly.

B. Mode characteristics

To understand the dipole coupling, we describe the modal profiles in detail in this section. As mentioned, the $\mathcal{PT}$-symmetric structure can operate in two regimes depending

on γ, separated by the EP located here at $\gamma_{EP} = 0.1231$ [Figs. 1(b) and 1(c)]. In the $\mathcal{PT}$-symmetric regime, the two supermodes propagate without any gain or loss, as shown by the real values of their propagation constants β. In the $\mathcal{PT}$-broken regime, one supermode experiences gain, shown by the positive imaginary part of β, while the other experiences losses, with a negative imaginary β. At the exceptional point, the modes merge and are defective: their propagation constants are equal, and the modes are proportional as will be shown later.

Depending on the value of the gain-loss parameter γ, the electric field profile of the supermodes exhibits different symmetries. As the electric dipole in our structure only has x and z components, we are mainly interested in the x and z electric field components of the modes [Fig. 1(f)]. We also detail the field characteristics at the position of the dipole $x = z = 0$ [Figs. 1(d) and 1(e)], as this will drive the dipole coupling (see further in Sec. III A). Note that the profiles of the modes are normalized according to the following orthonormalization relation using the unconjugated inner product:

$$\langle \mathbf{E}_m, \mathbf{H}_n \rangle = \iint_S (\mathbf{E}_m \times \mathbf{H}_n) \cdot \mathbf{u_z} dS = \delta_{mn}, \tag{1}$$

where $\mathbf{E}_m$ and $\mathbf{H}_n$ are the fields associated with modes m and n, respectively, S is a surface that encompasses a cross section of the structure cut perpendicularly to z, and $\mathbf{u}_z$ is a unit vector oriented along z [23,24].

For $\gamma = 0$, E_x is symmetric only for mode 1, while E_z is symmetric only for mode 2, the other mode having an antisymmetric profile [Fig. 1(f), $\gamma = 0$]. At the position of the source (0,0), this translates to a zero x field for mode 2 and a zero z field for mode 1 [Fig. 1(e), $\gamma = 0$]. Though the addition of a phase factor $e^{i\alpha}$ to the field components can arbitrarily mix the real and imaginary parts, we take as a convention a purely real $E_{1,x}$ and imaginary $E_{2,z}$ for $\gamma = 0$ in Fig. 1(f).

When $0 < \gamma < 0.1231$ ($\mathcal{PT}$-symmetric regime), E_x and E_z acquire a symmetric part for modes 2 and 1, respectively [Fig. 1(f), $\gamma = 0.05$]. Both modes then have one symmetric part for each field component: In our convention, the real parts of E_x and E_z for mode 1 and their imaginary parts for mode 2. At the source position, the x and z field components thus have an equal complex phase [Fig. 1(d)]. As a consequence, $E_{z,1}$ and $E_{x,2}$ become nonzero and get larger as γ increases and the symmetric parts of the field grow [Fig. 1(e)].

When $\gamma > 0.1231$ ($\mathcal{PT}$-broken regime), the electric fields of the two modes are asymmetric, with one mode being stronger in the gain guide and the other mode in the loss guide, but their profiles are simply mirrored with respect to $x = 0$ [Fig. 1(f), $\gamma = 0.15$] up to a change in sign. The x or z electric field components of modes 1 and 2 thus have equal modulus at the position of the dipole [Fig. 1(e)]. In our phase factor convention, the real parts of E_x and E_z are equal between modes 1 and 2 but their imaginary parts are opposite since they correspond to gain and loss modes: They are complex conjugates. At the source position, modes 1 and 2 therefore take opposite complex phase differences [Fig. 1(d)].

At the exceptional point, the orthogonality of the modes is lost and they become defective. As a consequence, their profiles are identical, up to a multiplicative constant. This can be seen in Fig. 1(f) closest to the EP, for $\gamma = 0.123$ and 0.124:

The electric field profile (x and z components alike) of mode 1 (blue) can be obtained by multiplying the profile of mode 2 (orange) by i. In our convention, their real (full line) and imaginary (dashed line) parts are simply interchanged, up to a change in sign.

Additionally, despite the mode profiles looking different in Fig. 1(f) just before and after the EP—antisymmetric or symmetric versus asymmetric—they are actually equivalent. The profile of a mode (1 or 2) at the inferior limit of the EP can be obtained by multiplying its profile at the superior limit by a complex number $(1 - i)\alpha$ where α is real. The transition between the regimes, the EP, is thus visible via this link between the profiles.

In the end, the analysis of the modes of the $\mathcal{PT}$-symmetric structure shows the expected regimes and the defectiveness at the EP, as well as various symmetries brought about by the geometry.

III. DIPOLE TAILORING

In order to create a contrast between the electromagnetic waves propagating on the left and right sides of the source, for each γ, we search for the electric dipole that provides an excitation amplitude closest to zero for a specific mode on the left side of the dipole, i.e., a highly directional excitation of that mode. We choose mode 2, as it is the gain mode in the $\mathcal{PT}$-broken regime ($\gamma > \gamma_{EP}$).

As shown later, after the EP, removing this mode on the left will therefore lead to gain only on the right. In the $\mathcal{PT}$-symmetric regime ($\gamma < \gamma_{EP}$), mode 2 is one of the two propagating supermodes of the structure. Thus, removing this mode on the left produces a uniform field profile, while exciting both modes on the right causes a beating, creating a different wave propagation between the sides.

To design a dipole that directionally excites the desired mode, one has to look into the theory behind the source-mode coupling.

A. Dipole source-mode coupling theory

The way a punctual source couples to the modes can be described analytically. The excitation amplitudes (A) of a mode—its contribution to the mode decomposition of the structure field—on (or towards) the left (l, $z < 0$) and right (r, $z > 0$) sides of a source are calculated using the following equations:

$$A_m^l \propto \vec{p}.\vec{E}_m^r(\vec{r}_0), \tag{2a}$$

$$A_m^r \propto \vec{p}.\vec{E}_m^l(\vec{r}_0), \tag{2b}$$

where $\vec{p}$ is the source dipole moment, $\vec{r}_0$ the position of the dipole, and $\vec{E}_m$ is the electric field associated to the mode with number m [23]. The electric field of a mode on the left or right of the source should not be confused with left and right eigenmodes of non-Hermitian systems. We do not distinguish these modes as they are proportional to each other, since we work in reciprocal media [25]. Their orthogonality is also guaranteed as the unconjugated inner product [Eq. (1)] is used in the orthonormalization [23,26].

According to the Maxwell equations, if we define the field of a mode m propagating towards $z > 0$ as

$(E_{m,n}, E_{m,z}, H_{m,n}, H_{m,z})$, the subscript n referring to components normal to z, the field of the same mode m propagating towards $z < 0$ is $(E_{m,n}, -E_{m,z}, -H_{m,n}, H_{m,z})$. We define $E_{m,x}$ and $E_{m,z}$ as the field components of the right-side mode ($z > 0$) at the dipole position $\vec{r}_0$ and develop the scalar products of Eqs. (2):

$$A_m^l \propto p_x E_{m,x} + p_z E_{m,z}, \tag{3a}$$

$$A_m^r \propto p_x E_{m,x} - p_z E_{m,z}. \tag{3b}$$

A mode m will therefore only be excited by an x- or z-oriented dipole if $E_{m,x}$ or $E_{m,z}$, respectively, are nonzero at the position of the dipole.

By setting A_m^l or A_m^r to 0, Eqs. (3) show that a mode m can be excited on one side while being canceled on the other side if

$$p_x E_{m,x} = \pm p_z E_{m,z}. \tag{4}$$

The mode will be canceled on the left side in the $-$ case and on the right side in the $+$ case.

Since in our structure the modes can have complex electric fields, we replace the complex components p_x, $E_{m,x}$, p_z, and $E_{m,z}$ by their polar expressions $|p_x|e^{i\phi_{px}}$, $|E_{m,x}|e^{i\phi_{Ex}}$, $|p_z|e^{i\phi_{pz}}$, and $|E_{m,z}|e^{i\phi_{Ez}}$ in Eq. (4). The condition to cancel the mode m then becomes

$$|p_x|e^{i\phi_{px}}|E_{m,x}|e^{i\phi_{Ex}} = \pm|p_z|e^{i\phi_{pz}}|E_{m,z}|e^{i\phi_{Ez}}, \tag{5}$$

which is fulfilled if

$$|p_x||E_x| = |p_z||E_z| \text{ and } \phi_{px} - \phi_{pz} = \phi_{Ez} - \phi_{Ex}(+\pi), \tag{6}$$

where π needs to be added if one cancels the mode on the left side.

These conditions can be viewed geometrically by returning to the formulation of Eq. (2): a mode m will be canceled on the left if $\vec{p} \cdot \vec{E}_m^l = 0$, that is if the dipole and the field are orthogonal. This orthogonality of the vectors is exactly expressed by the conditions in Eq. (6). Canceling a mode with a linear electric field will thus require the use of a linear dipole perpendicular to the field, and an elliptical field requires a dipole of matching ellipticity also perpendicular to the field.

B. Dipole-mode coupling in the $\mathcal{PT}$ structure

According to the theory, the coupling of a given dipole to the modes of a photonic structure practically only depends on the field of the modes at the position of the dipole. As a result, the peculiar symmetries of the modes of our $\mathcal{PT}$-symmetric structure, described in Sec. II B, create special couplings with a dipolar source placed in the center of the structure ($x = 0$). These tendencies are summarized in Figs. 2(a) and 2(b) for an x- and z-dipole, respectively. These figures also show that, around the EP, the excitation amplitude of the modes increases, which is reminiscent of the Purcell effect in $\mathcal{PT}$ structures [25]. The excitation of the modes by the x and z dipole components then need to be considered together when adapting the dipole to respect the condition for contrast [Eq. (4)]. The tailored dipole characteristics, which for every γ eliminate mode 2 on the left side, are presented in Fig. 2(c).

When $\gamma = 0$, at the position of the dipole E_x is only nonzero for mode 1, and E_z is nonzero only for mode 2. Consequently, the x dipole excites only mode 1, and the z dipole
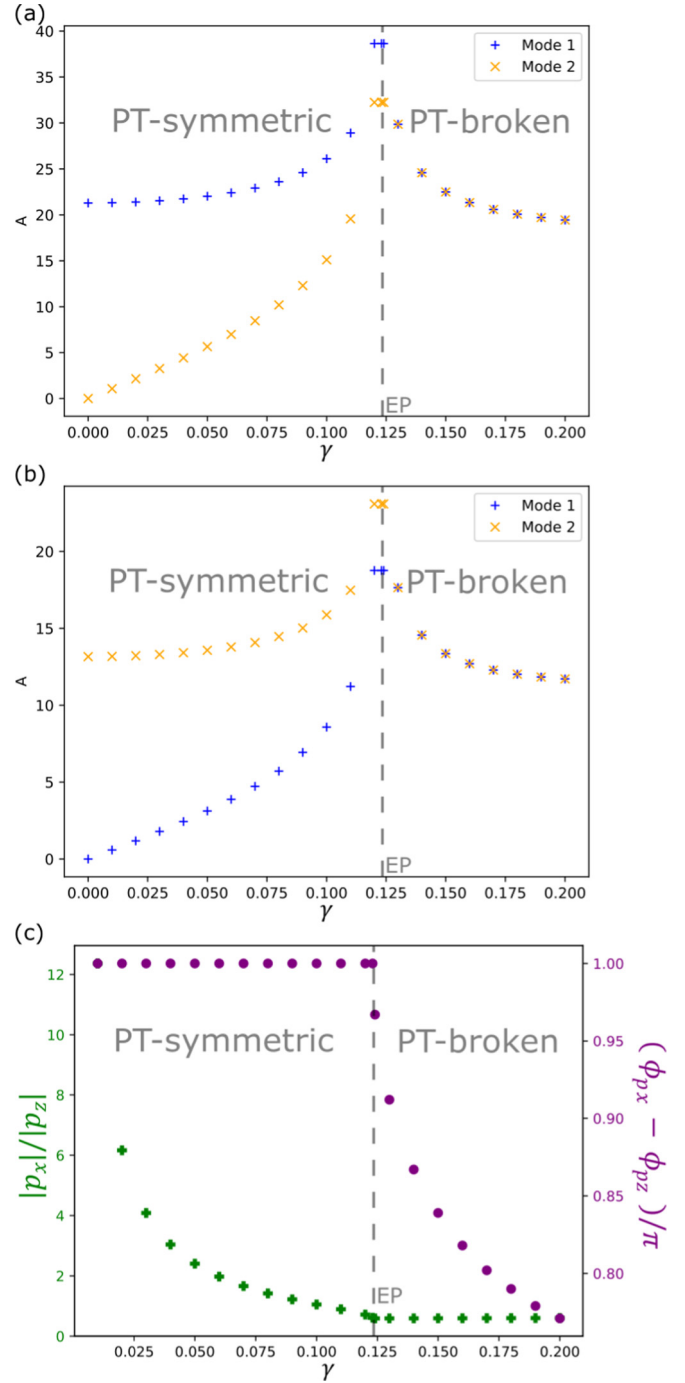

FIG. 2. (a), (b) Excitation amplitudes of modes 1 (blue) and 2 (orange) by an (a) x- or (b) z-oriented dipole as a function of the gain-loss parameter γ. (c) Characteristics of the dipole tailored for the desired contrast at each γ. The exceptional point is located at $\gamma_{EP} = 0.1231$ and marked by a gray dashed line.

only mode 2 [Figs. 2(a) and 2(b)]. Obtaining a directionality in these conditions is impossible. In order to cancel mode 2 on the left, the z dipole cannot be used. As seen in Eq. (4), since $E_{2,x} = 0$ the left-hand side of the equation cancels. To satisfy the equation, p_z thus needs to be 0 to cancel the right-hand side. However, both $p_z E_{2,z}$ and $p_x E_{2,x}$ are then zero, which
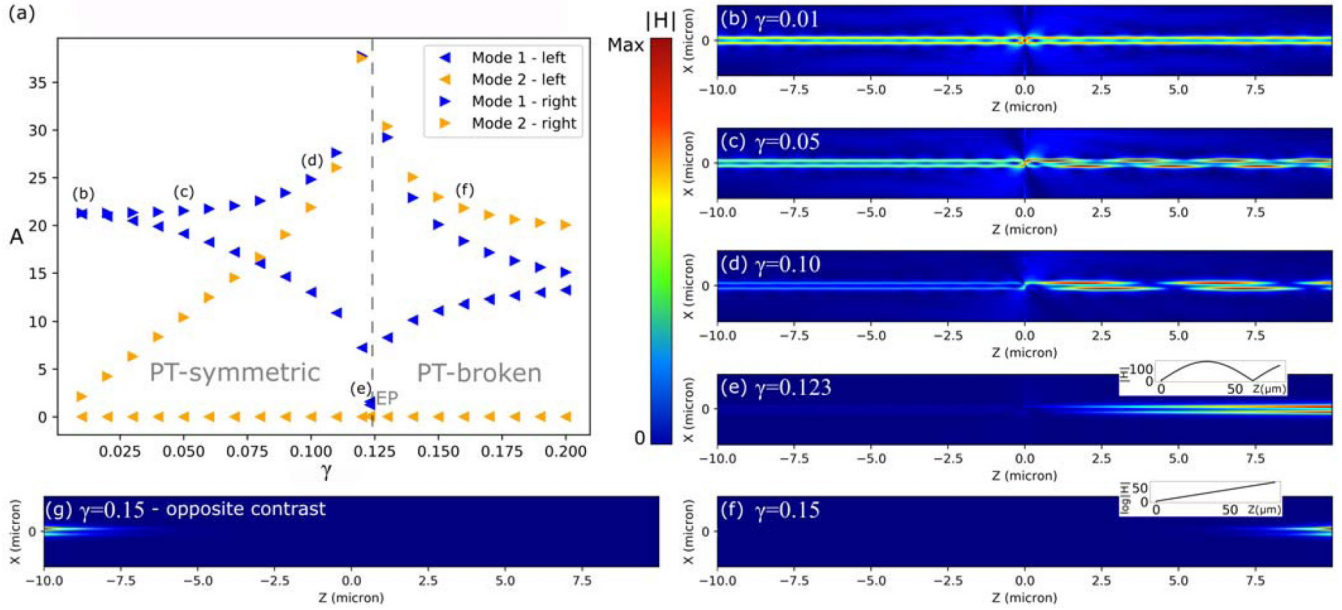
FIG. 3. (a) Excitation amplitude of modes 1 (blue) and 2 (orange) on each side of the dipole tailored for left-right contrast for values of the gain-loss parameter $\gamma = 0.01$ to 0.20. The exceptional point is located at $\gamma_{EP} = 0.1231$ and marked by a gray dashed line. (b)-(f) Magnetic field absolute value in the structure for $\gamma = 0.01, 0.05, 0.10, 0.123$, and 0.15, respectively. The dipole is at the center (0,0), the gain waveguide on the top and the loss waveguide on the bottom, as in Fig. 1(a). In these images, the tailored dipoles are used, with mode 2 canceled on the left side. The insets in (e) and (f) represent (e) the absolute magnetic field or (f) its logarithm in the center of the gain guide for $z = 0$ to 80 μm. (g) Magnetic field absolute value in the structure for $\gamma = 0.15$, with mode 2 canceled on the right side instead of the left. The dipole tailored for $\gamma = 0.15$ is used, with an added phase of π compared to image (f).

fulfills the conditions to cancel the mode on both sides of the dipole, giving no left-right contrast.

In the $\mathcal{PT}$-symmetric regime, both modes have one symmetric part for E_x and E_z, meaning that both dipole components can now excite both modes. The values of the field are different for modes 1 and 2, since the symmetric parts of the field components evolve differently for these two modes (see Fig. 1). For a given value of γ, the ratio between the x and z components of the dipole thus has to be adjusted to fulfill the condition in Eq. (6) ($|p_x|/|p_z| = |E_z|/|E_x|$), which explains the variation of $|p_x|/|p_z|$ in Fig. 2(c).

When it comes to the relative phase of the dipole components, we saw in Fig. 1(d) that $\phi_{Ez} - \phi_{Ex} = 0$ for both modes. The condition on the dipole that naturally results from these mode characteristics is that $\phi_{px} - \phi_{pz} = \pi$ in order to cancel a mode on the left, as seen in Fig. 2(c). The selection of mode 2 as the one to be canceled is done through the choice of the adequate ratio of $|p_x|$ and $|p_z|$. Geometrically, the electric field of the modes is linear in this regime and therefore requires a *linear* dipole $\vec{p}$ perpendicular to their field $\vec{E}$ to be canceled. The variation in $|p_x|/|p_z|$ assures the adaption of the dipole orientation to that of the electric field $\vec{E}$ as γ increases up to the EP.

In the $\mathcal{PT}$-broken regime, it can be seen in Figs. 2(a) and 2(b) that the excitation amplitudes of modes 1 and 2 are equal for the same dipole (identical blue and orange results). This is also explained by Eqs. (2). Because modes 1 and 2 are asymmetric but mirrored with respect to $x = 0$, they have equal values of $|E|$ at the source, resulting in equal excitations of the two modes. For each $\gamma > \gamma_{EP}$, the ratio $|p_x|/|p_z|$ still is $\neq 1$ as $|E_x| \neq |E_z|$, and it needs to be slightly adjusted to

account for the change in $|E_z|/|E_x|$ [see Eq. (6) and Figs. 2(a) and 2(b)].

Since in this regime the relative phase of the field components $\phi_{Ez} - \phi_{Ex}$ also varies, the relative phase of the dipole components needs to be adjusted. For mode 2, it can be seen in Fig. 1(d) that $\phi_{Ez} - \phi_{Ex}$ becomes <0 as γ increases, so $\phi_{px} - \phi_{pz}$ needs to become $< \pi$. These trends in the dipole characteristics are shown in the right part of Fig. 2(c).

Geometrically, as γ increases beyond the EP the electric field of the modes at the source becomes increasingly more elliptical, as opposed to linear in the $\mathcal{PT}$-symmetric regime. To maintain the orthogonality between $\vec{p}$ and $\vec{E}_m$, the dipole thus needs to match that ellipticity through the variation of $\phi_{px} - \phi_{pz}$, while adapting its orientation with $|p_x|/|p_z|$.

IV. AMPLITUDE CONTRAST

After determining the dipole with the desired directionality for each γ, we extract the excitation amplitudes of modes 1 and 2 on the two sides of each dipole, and represent them as a function of γ in Fig. 3(a).

Figure 3(a) clearly shows that each tailored dipole excites mode 2 with an amplitude close to zero on the left side. Figures 3(b)–3(f) indicate the resulting profiles for wave propagation on both sides of the dipole. A qualitative change between the $\mathcal{PT}$-symmetric ($\gamma < 0.1231$) and the $\mathcal{PT}$-broken ($\gamma > 0.1231$) regimes is observed.

In the $\mathcal{PT}$-symmetric regime [Fig. 3(a), $\gamma < 0.1231$, and Figs. 3(b)–3(d)], for all values of γ, a beating appears on the right side of the dipole, while the left side is the excitation of a single supermode. Any residual fluctuations on the left are the

result of radiative modes that are not perfectly absorbed at the top and bottom edges of the simulation domain with perfectly matched layers.

Furthermore, the field profile in the structure changes when the amount of gain-loss γ varies. For small values of γ, mode 1 is more strongly excited than mode 2 on both sides, resulting in a similar strength of the field on both sides [Fig. 3(b), $\gamma = 0.01$]. Then, when γ gets closer to the EP [Figs. 3(c) and 3(d), $\gamma = 0.05$ and 0.10], the mode 1 excitation amplitude on the left keeps decreasing while mode 2 on the right gets stronger; the field thus becomes larger on the right side (with stronger beatings, that become more "tilted" as there are power oscillations).

At the exceptional point $\gamma = 0.1231$, the modes merge, as mentioned in Sec. II. The excitation amplitude of modes 1 and 2 must then be equal on each side. Since mode 2 is canceled on the left, mode 1 is as well, and the field becomes near zero on this side. On the right side, both modes remain strong, and a beating still occurs right before the theoretical EP [Fig. 3(e)]. As a result a near-complete directionality is achieved close to the EP using the tailored dipole polarization, which is reminiscent of the situation with only one (super)mode on each side.

When γ increases further to enter the $\mathcal{PT}$-broken regime, the excitation amplitude of the modes on the right starts to decrease, showing the change in regime [Fig. 3(a), $\gamma > 0.1231$]. The absence of mode 2 on the left while still being excited on the right causes a strong contrast, as it is the gain mode: The field increases exponentially on the right of the dipole; see Figs. 3(f). On the left side of the dipole, mode 1 also starts to increase with γ, but the field stays larger on the right side as mode 1 is the lossy mode.

Furthermore, for any γ, in both regimes, the directional excitation can be switched between the two sides by adding a phase of π to the phase difference between the components of the adequate dipole [see Figs. 3(f) and 3(g)]. This change in phase can be obtained by assigning an opposite phase to one of the components of the dipole (x or z).

Until now we have reported results on a source that was tailored for all γ values, to clearly show the behavior. It is interesting to note that one can also use a source tailored for only a specific γ, which could be easier experimentally. In that case one obtains the contrast for a specific gain-loss value, so no beating if this value is before the EP, and gain on one side if this value is above the EP. Other γ values then lead to the "standard" phenomena: Beating profiles (below EP) and gain (above EP) on both sides.

V. CONCLUSION

We highlight the peculiar properties of the modes of two coupled $\mathcal{PT}$-symmetric waveguides in both symmetric and broken regimes. The coupling mechanism of an electric dipole to these modes is theoretically reviewed, and applied to our structure, in order to obtain a condition for directional mode excitation. By tailoring the polarization of a dipole to the properties of $\mathcal{PT}$-modes, the desired directionality is achieved for all nonzero values of the gain-loss parameter γ. This creates a left-right contrast in the wave propagation in the structure,

with the presence of either beating ($\gamma < \gamma_{EP}$) or field amplification ($\gamma > \gamma_{EP}$) on a chosen side of the dipole. Our results also highlight a feature of the EP: the defectiveness of the modes in this unique configuration enables a near-complete directional excitation.

In addition, we find that a well-positioned linear dipole can be used to cancel a specific mode in the $\mathcal{PT}$-symmetric regime ($\gamma < \gamma_{EP}$). Though the field of the modes is generally elliptic, in the center of the two waveguides it is linear due to the $\mathcal{PT}$ symmetry of the modes, allowing the use of a linear dipole instead of an elliptic one to create the directionality. If the dipole were placed off-center, closer to one of the waveguides, the electric field of the $\mathcal{PT}$-symmetric modes would be elliptical. The left-right contrast presented in this work could still be achieved, but a perpendicular elliptical dipole of matching ellipticity would then be required, as in the $\mathcal{PT}$-broken regime. Nevertheless, the directionality is relatively robust to small dipole displacements: we checked that a significant mode cancellation is still achieved when a dipole tailored for the center position is used at a slightly off-center position. A similar robustness to small gain-loss imbalances has also been observed.

The various types of contrast shown in Sec. IV can be used for applications in integrated photonics. The presence of beating on one selected side of the dipole in the $\mathcal{PT}$-symmetric regime could be used in a directional coupler arrangement, so with four ports, and the dipole between the waveguides in the coupling section. As the structure is also longitudinally invariant, the dipole could be moved along the propagation direction in the directional coupler arrangement to shift the field profile and excite either the top or the bottom port waveguide. With one structure, any of the four ports of the coupler can be selectively excited, only by changing the position or the polarization of the source.

For γ close to the EP [for example, Fig. 3(e)], the two modes are almost defective, so they are practically equally excited. In essence, this is a particular point with a behavior similar to a dipole near a *single* waveguide. As seen in Fig. 3(a), both modes are almost not excited on the left side in these conditions, while they are strongly excited on the right side. At the EP, fully directional excitation is thus possible. At other values of γ, both modes could be canceled simultaneously if the right conditions were met, but it would require a specific configuration of the mode profiles and the dipole, which is unlikely to be achieved without optimizing the structure.

In the $\mathcal{PT}$-broken regime, various left-right amplitude contrasts can be obtained. By adjusting the source polarization, the field amplification can be set to either appear only on the left or right [directionality, as seen in Figs. 3(f) and 3(g)] or be balanced between the two sides (no directionality). This tunable contrast could find applications in lasing and routing photonic structures.

[1] F. J. Rodríguez-Fortuño, G. Marino, P. Ginzburg, D. O'Connor, A. Martínez, G. A. Wurtz, and A. V. Zayats, Near-field interference for the unidirectional excitation of electromagnetic guided modes, Science **340**, 328 (2013).

[2] M. F. Picardi, A. V. Zayats, and F. J. Rodríguez-Fortuño, Janus and Huygens Dipoles: Near-Field Directionality beyond Spin-Momentum Locking, Phys. Rev. Lett. **120**, 117402 (2018).

[3] A. Aiello, P. Banzer, M. Neugebauer, and G. Leuchs, From transverse angular momentum to photonic wheels, Nat. Photonics **9**, 789 (2015).

[4] A. Espinosa-Soria and A. Martínez, Transverse spin and spin-orbit coupling in silicon waveguides, IEEE Photonics Technol. Lett. **28**, 1561 (2016).

[5] S. Perea-Puente and F. J. Rodríguez-Fortuño, Dependence of evanescent wave polarization on the losses of guided optical modes, Phys. Rev. B **104**, 085417 (2021).

[6] B. le Feber, N. Rotenberg, and L. Kuipers, Nanophotonic control of circular dipole emission, Nat. Commun. **6**, 6695 (2015).

[7] A. G. Lamprianidis, X. Zambrana-Puyalto, C. Rockstuhl, and I. Fernandez-Corbaton, Directional coupling of emitters into waveguides: A symmetry perspective, Laser Photonics Rev. **16**, 2000516 (2022).

[8] M. Channab, C. F. Pirri, and A. Angelini, Funneling spontaneous emission into waveguides via epsilon-near-zero metamaterials, Nanomaterials **11**, 1410 (2021).

[9] W.-S. Ruan, X.-T. He, F.-L. Zhao, and J.-W. Dong, Analysis of unidirectional coupling in topological valley photonic crystal waveguides, J. Lightwave Technol. **39**, 889 (2021).

[10] L. Feng, R. El-Ganainy, and L. Ge, Non-hermitian photonics based on parity-time symmetry, Nat. Photonics **11**, 752 (2017).

[11] C. Rüter, K. Makris, R. El-Ganainy, D. Christodoulides, M. Segev, and D. Kip, Observation of parity-time symmetry in optical systems, Opt. Photonics News **21**, 47 (2010).

[12] H. Benisty, A. Degiron, A. Lupu, A. D. Lustrac, S. Chénais, S. Forget, M. Besbes, G. Barbillon, A. Bruyant, S. Blaize, and G. Lérondel, Implementation of PT symmetric devices using plasmonics: Principle and applications, Opt. Express **19**, 18004 (2011).

[13] *Parity-Time Symmetry and Its Applications*, edited by D. Christodoulides, J. Yang, Springer Tracts in Modern Physics (Springer, Singapore, 2018), Vol. 280.

[14] H. Ramezani, T. Kottos, R. El-Ganainy, and D. N. Christodoulides, Unidirectional nonlinear $\mathcal{PT}$-symmetric optical structures, Phys. Rev. A **82**, 043803 (2010).

[15] R. Kolkowski and A. F. Koenderink, Lattice resonances in optical metasurfaces with gain and loss, Proc. IEEE **108**, 795 (2020).

[16] J. Petráček, Nonreciprocal transmission in coupled nonlinear waveguides with loss and gain, in *2017 19th International Conference on Transparent Optical Networks (ICTON)* (2017), pp. 1–4.

[17] A. Lupu, H. Benisty, and A. Degiron, Switching using PT symmetry in plasmonic systems: Positive role of the losses, Opt. Express **21**, 21651 (2013).

[18] P. Markoš and V. Kuzmiak, Resonant scattering from a two-dimensional honeycomb $\mathcal{PT}$ dipole structure, Phys. Rev. A **97**, 053807 (2018).

[19] H. Hodaei, A. Hassan, S. Wittek, H. Garcia-Gracia, R. El-Ganainy, D. Christodoulides, and M. Khajavikhan, Enhanced sensitivity at higher-order exceptional points, Nature (London) **548**, 187 (2017).

[20] M.-A. Miri and A. Alù, Exceptional points in optics and photonics, Science **363**, eaar7709 (2019).

[21] I. Katsantonis, S. Droulias, C. M. Soukoulis, E. N. Economou, and M. Kafesaki, Scattering properties of PT-symmetric chiral metamaterials, Photonics **7**, 43 (2020).

[22] Y. D. Chong, L. Ge, and A. D. Stone, $\mathcal{PT}$-symmetry breaking and laser-absorber modes in optical scattering systems, Phys. Rev. Lett. **106**, 093902 (2011).

[23] P. Bienstman, Rigorous and efficient modelling of wavelength scale photonic components, Ph.D. thesis, Universiteit Gent, 2001.

[24] P. Bienstman and R. Baets, Optical modelling of photonic crystals and vcsels using eigenmode expansion and perfectly matched layers, Opt. Quantum Electron. **33**, 327 (2001).

[25] A. Pick, B. Zhen, O. D. Miller, C. W. Hsu, F. Hernandez, A. W. Rodriguez, M. Soljač ić, and S. G. Johnson, General theory of spontaneous emission near exceptional points, Opt. Express **25**, 12325 (2017).

[26] M. Skorobogatiy, Hamiltonian formulation of Maxwell equations for the modes of anisotropic waveguides, in *Nanostructured and Subwavelength Waveguides* (John Wiley & Sons, New York, 2012), pp. 21–37.